Published in final edited form as:
J Control Release. 2012 May 10; 159(3): 393–402. doi:10.1016/j.jconrel.2012.01.009.

Liposomes Loaded with Paclitaxel and Modified with Novel Triphenylphosphonium-PEG-PE Conjugate Possess Low Toxicity, Target Mitochondria and Demonstrate Enhanced Antitumor Effects *In Vitro* and *In Vivo*

Swati Biswas, **Namita S. Dodwadkar**, **Pranali P. Deshpande**, and **Vladimir P. Torchilin***
Center for Pharmaceutical Biotechnology and Nanomedicine, 360 Huntington Avenue, 312 Mugar Hall, Northeastern University, Boston, Massachusetts 02115.

Abstract

Previously, stearyl triphenylphosphonium (STPP)-modified liposomes (STPP-L) were reported to target mitochondria. To overcome a non-specific cytotoxicity of STPP-L, we synthesized a novel polyethylene glycol- phosphatidylethanolamine (PEG-PE) conjugate with the TPP group attached to the distal end of the PEG block (TPP-PEG-PE). This conjugate was incorporated into the liposomal lipid bilayer, and the modified liposomes were studied for their toxicity, mitochondrial targeting, and efficacy in delivering paclitaxel (PTX) to cancer cells *in vitro* and *in vivo*. These TPP-PEG-PE-modified liposomes (TPP-PEG-L), surface grafted with as high as 8 mole % of the conjugate, were less cytotoxic compared to STPP-L or PEGylated STPP-L. At the same time, TPP-PEG-L demonstrated efficient mitochondrial targeting in cancer cells as shown by confocal microscopy in co-localization experiments with stained mitochondria. PTX-loaded TPP-PEG-L demonstrated enhanced PTX-induced cytotoxicity and anti-tumor efficacy in cell culture and mouse experiments compared to PTX-loaded unmodified plain liposomes (PL). Thus, TPP-PEG-PE can serve as a targeting ligand to prepare non-toxic liposomes as mitochondria-targeted drug delivery systems (DDS).

Keywords

Liposomes; amphiphilic polymer; PEG-PE; mitochondrial targeting; TPP; cancer; anti-tumor; paclitaxel

1. Introduction

Organelle-specific targeting of bio-active molecules is important to achieve maximum therapeutic and minimum side-effects [1]. Pharmaceutical agents, if directed specifically towards the organelle of interests, such as nucleic acid materials to the nuclei, pro-apoptotic compounds to the mitochondria and lysosomal drugs to the lysosomes could enhance their therapeutic effect manifold compared to the random interactions with the desired site of

*Corresponding author: Vladimir P. Torchilin, Ph.D., D.Sc., Center for Pharmaceutical Biotechnology and Nanomedicine, Northeastern University, 312 Mugar Hall, 360 Huntington Ave., Boston, Massachusetts 02115, v.torchilin@neu.edu, Phone. 617-373-3206, Fax. 617-373-7509.

action [2–6]. However, directing intracellular trafficking of bio-actives to the organelles of interest represent major challenge for drug delivery. To achieve intracellular targeting, one option is to modify the drug molecule with organelle-specific ligands, which could however result in a compromised drug effect. Another option is to modify a drug-loaded DDS, such as liposomes, to direct it to a specific organelle.

In recent years, mitochondrial targeting of small molecules/nanocarriers has gained much attention because of the progressive evidence that mitochondrial dysfunction is responsible for a variety of human disorders including neurodegenerative, neuromuscular diseases, diabetes, obesity and cancer [7–11]. Mitochondria also happen to be the key regulators of apoptosis [3, 12–14] by triggering the complex cell-death processes by a variety of mechanisms including translocation of the pro-apoptotic proteins such as cytochrome-*C*, apoptosis-inducing factor from the mitochondrial inter-membrane space to the cytosol, which then activate the death-signal proteins such as caspases [15, 16]. Since the mitochondria play a pivotal role in cell-death, a mitochondria-targeted treatment strategy could be promising for cancer therapy [17]. Thus, there is increasing evidence that the cytotoxic effect of the potent chemotherapeutic drug PTX is mediated through mitochondria. In addition to stabilizing microtubules by interacting with β-tubulin, PTX directly binds to the anti-apoptotic protein Bcl-2 in mitochondria, mimicking the binding motif as its ligand orphan nuclear receptor Nur77, thereby facilitating the initiation of apoptosis by converting Bcl-2 from anti-apoptotic to pro-apoptotic which opens the mitochondrial permeability transition pore (mPTP) channels [18–20]. PTX has been shown to depolarize mitochondria and induce mPTP with subsequent initiation of apoptosis [21]. Therefore, targeting PTX towards mitochondria should result in an enhanced therapeutic effect.

To achieve mitochondrial targeted delivery, the large membrane potential across mitochondrial inner membrane is utilized [22, 23]. Lipophilic cations, such as triphenylphosphonium (TPP) accumulate in the mitochondrial matrix [22, 24]. Modification of small molecules with a TPP group enhances mitochondrial targeting [25–28]. Surface modification of nanoparticular DDS with various mitochondriotropic ligands, such as lipophilic cations, mitochondrial protein import machinery, mitochondrial targeting signal peptides, makes nanocarriers mitochondriotropic [28–32]. A recently developed amphiphilic polyproline cell penetrating agent is able to locate inside the mitochondria [23]. Previously, the TPP group was conjugated to the non-polar stearyl moiety, and the resultant STPP was incorporated into the lipid bilayer of the liposomes. These STPP-L have been shown to accumulate in mitochondria and were efficient in delivering the anti-cancer drugs sclareol and ceramide, to the mitochondria [32–34]. However, the non-specific toxicity of the nanocarrier represents a major challenge.

In the present study, in an attempt to prepare a non-toxic mitochondria-targeted DDS, we synthesized a novel TPP-conjugated PEG-PE polymer (TPP-PEG-PE) and incorporated it into the liposomes. We assumed that the TPP-group attached to the liposome via PEG chain would more readily interact with mitochondria compared to the membrane-embedded ligand. The cytotoxicity of TPP-PEG-PE and various STPP-modified liposomes were determined as well as the efficacy of mitochondria-targeted drug-loaded TPP-L compared to PL. TPP-PEG-L were used to deliver PTX to the mitochondria of cancer cells (HeLa and 4T1) in an attempt to enhance the PTX-mediated cytotoxicity. Finally, the anti-tumoral efficacy of PTX-loaded TPP-PEG-L was evaluated *in vivo* in 4T1-tumor-bearing mice.

2. Materials and Methods

2.1. Materials

1,2-Distearoyl-*sn*-glycero-3-phosphoethanolamine-*N*-[methoxy (polyethylene glycol)-2000] (PEG-$_{2K}$-PE), 1,2-dimyristoyl-*sn*-glycero-3-phosphoethanolamine-*N*-(lissamine rhodamine B sulfonyl) (ammonium salt, Rh-PE), egg L-α-phosphatidylcholine (ePC), 1,2-distearoyl-*sn*-glycero-3-phophoethanolamine-*N*-[amino(polyethylene glycol)2000] (ammonium salt) (NH_2-PEG-PE) were purchased from Avanti Polar Lipids Inc. (Alabaster, AL) and used without further purification. Cholesterol, chloroform-*d*, (3-carboxypropyl)triphenyl-phosponium bromide (CTPP), paclitaxel, N-(3-dimethylaminopropyl)-N'-ethylcarbodiimide hydrochloride (EDCI), N-hydroxysuccinimide (NHS) and triethylamine (TEA) were purchased from Sigma (St Louis, MO). Stearyl bromide and cellulose ester (CE) dialysis membrane 2000Da MWCO were purchased from Fisher Scientific (Fair Lawn, NJ). Para-formaldehyde was purchased from Electron Microscopy Sciences (Hatfield, PA). Fluoromount-G was from Southern Biotech (Birmingham, AL). The CellTiter 96® AQueous One Solution Cell Proliferation Assay kit was purchased from Promega (Madison, WI). FragEL™ DNA Fragmentation Detection Kit, Fluorescent-TdT enzyme was obtained from EMD Biosciences. All fluorescence dyes used in this study were obtained from Molecular Probes.

2.2. Synthesis of mitochondriotropic polymer TPP-PEG-PE

Into a solution of 9.2 mg (21.4 μM) of CTPP in 1 mL of chloroform, 20 μL of triethylamine, 12.4 mg (64.5 μM) of EDCI and 7.4 mg (64.5 μM) of NHS were added. The mixture was stirred at room temperature (RT) for 2 h before addition of 50 mg of NH_2-PEG-PE in chloroform (25 mg/mL). The reaction mixture was stirred overnight at RT under nitrogen, and chloroform was evaporated. The crude reaction mixture was diluted with water and dialyzed against water using cellulose ester membrane of 2 KDa MWCO for 24 h. The dialysate was freeze-dried to obtain pure TPP-PEG-PE polymer (yield 50 mg, 90 %). The polymer was dissolved in chloroform at a concentration of 10 mg/mL and kept at −80 °C for future studies. The polymer was dissolved in chloroform-*d* and analyzed by ^{1}H-NMR using a Varian 500 MHz spectroscope. STPP was prepared following the previously published procedure [32, 33].

2.3. Preparation and characterization of liposomes

2.3.1. Preparation of liposomes—TPP-PEG-L, STPP-L, and PL were prepared with a lipid composition of ePC, cholesterol, TPP-PEG-PE or PEG-PE or STPP in a molar ratio of (70-x):30:x respectively where x was the mole % of the TPP-PEG-PE, PEG-PE or STPP component (table 1). In some liposomal preparations, a fraction of ePC was replaced with other lipid components, while the cholesterol mole % was kept constant. For cytotoxicity experiments, STPP+PEG-L was prepared using 8 mole % of STPP with 8 mole % of PEG-2000-PE. Table 1 represents the lipid composition of all liposomes. Three liposomes containing 3, 5 and 8 mole % of TPP-PEG-PE were used for initial cell-uptake studies. For flow cytometry analysis and microscopic visualization, the liposomes contained rhodamine PE as a fluorescent lipid marker by replacing 0.5 mole % of ePC from the lipid composition.

Liposomes were prepared by the lipid film hydration technique [35]. In brief, a dry lipid film was prepared in a round bottom flask by rotary evaporation of the chloroform solution of the combined lipid ingredients, followed by freeze-drying (Labconco Freeze Dry System, Freezone) for at least 1 h to remove the traces of solvents. The dry lipid film was hydrated with PBS, pH 7.4, and vortexed until all components were dissolved. The final lipid concentration was 4 mg/mL. The lipid solution was then extruded 20 times through a 200-

nm pore-sized polycarbonate membrane filter (Avanti Polar Lipids Inc.) to yield liposomes of a uniform particle size.

For the preparation of PTX-loaded TPP-PEG-L and PL, a PTX stock solution in methanol (0.5 mg/mL) was added to the lipid mixture in chloroform at the concentration of 1 % w/w of the amount of ePC. Liposomes were prepared following the above mentioned procedures. The non-incorporated PTX was removed by centrifugation of liposomes at 2000 rpm for 10 min, which precipitated the free PTX. PTX content was determined by HPLC.

2.3.2. Physico-chemical characterization of liposomes—The size and size distribution of liposomes were measured by the dynamic light scattering (DLS) using a Zeta Plus instrument (Brookhaven Instrument Corporation, Holtsville, NY). The zeta potential of liposomes was measured by a zeta phase analysis light scattering (PALS) system with an ultra-sensitive zeta potential analyzer. The liposome suspensions were diluted as needed in water or a 1 M KCl solution.

2.3.3. Measurement of PTX-loading in liposomes—The amount of PTX in TPP-PEG-L and PL was determined by the reverse phase HPLC (D-7000 HPLC system, Hitachi, Japan) using an Xbridge column (C_{18}, 4.6 mm, 250 mm, Waters, Milliford, MA). An aliquot of liposomes was dissolved in a solvent mixture of acetonitrile:water (7:3) and then injected into the HPLC system using acetonitrile:water (7:3) as the mobile phase at the flow rate of 1 mL/min with the detection at 227 nm. Each run was done in triplicate. The PTX loading in the liposomes was determined from the AUC with a calibration curve (AUC vs concentration of PTX solution (μg/mL) injected), obtained in the same conditions.

$$\%\ \text{of PTX}-\text{loading}=\frac{\text{Amount of PTX in liposomes obtained by HPLC analysis}}{\text{Amount of PTX}-\text{added at the time of liposome}-\text{preparation}}\times 100$$

2.4. Cell Culture

The human cervical cancer cell line (HeLa) and mouse mammary carcinoma cells (4T1) were purchased from the ATCC (American Tissue Culture Collection, Manassas, VA) and cultured in Dulbecco's Modified Eagles Medium (DMEM, Invitrogen), supplemented with 10 % fetal bovine serum (Gibco), 100 IU/mL penicillin, and 100 μg/mL streptomycin (Invitrogen) in a humidified air with 5 % CO_2 at 37 °C.

2.5. Cytotoxicity of empty liposomes

5×10^3 HeLa cells/well were seeded in 96-well cell culture plates. Next day, the cells were incubated with various liposomal formulations including TPP-PEG-L (8 %), STPP-L (1.5 %), STPP+PEG-L (8 % STPP and 8 % PEG-$_{2K}$-PE), and STPP-L (8 %) at lipid concentrations ranging from 0 to 500 μg/mL for 24 h. Cells were washed with PBS, and the cytotoxicity was evaluated by the Cell Titer Blue assay following the manufacturer's protocol. Percent cell viability was plotted as a function of total lipid concentration (μg/mL).

2.6. Quantification of cellular uptake of modified liposomes by flow cytometry

To assess the cell association of PL and TPP-PEG-L, a time-dependent flow cytometry analysis was performed using Rh-labeled liposomes containing a varied mole % of TPP-PEG-PE and PEG-PE (3.5 and 8). HeLa cells were seeded in 6-well tissue culture plates (Corning, NY, USA) at 5×10^4 cells/well. After one day, cells were incubated with liposomes at a lipid concentration of 100 μg/mL for 1 and 4 h in serum free DMEM at 37°C. Each data point was collected in triplicate. After the incubation, cells were washed twice with ice-cold PBS, detached by gentle scrapping, collected in 15 mL tubes and centrifuged at 1000 RPM

for 5 mins at 4°C to obtain a cell pellet. The cells were re-suspended in PBS. The samples were kept on ice until cell-association of Rh-labeled liposomes was evaluated using a BD FACS Caliber flow cytometer, equipped with 550 nm laser. The cells were gated using forward versus side scatter to exclude debris and dead cells before analyzing by FACS with 10,000 cell counts. The data were analyzed with BD Cell Quest Pro software.

2.7. Mitochondrial targeting by Confocal Laser Scanning Microscopy (CLSM)

HeLa cells were grown to 30–40 % confluence on 22-mm cover slips in 6-well cell culture plates. Cells were exposed to Rh-PE-labeled PL and TPP-PEG-L for 18 h in darkness in complete medium. At the end of the incubation period, cover slips were washed at least 4 times with PBS, pH 7.4. The cells were incubated in a serum-free media in the presence of Mitotracker Green (MTG, Molecular Probes, Eugene, OR) at a concentration of 100 nM for 30 min for mitochondrial staining, and Hoechst 33342 at 5 μg/mL for 5 min for nuclear staining. The cells were washed several times with PBS. The cover slips were mounted on Fluoromount-G medium and examined on a Confocal Zeiss LSM 700 microscope with filters set at 365 ± 5 nm excitation light for Hoechst 33342, 470 ± 20 nm for MTG, and 535 ± 25 nm excitation light for Rh-PE labeled liposomes. Zeiss ZEN 2009 software was used for set up and Image *J* software was used for image processing. Fluorescence from the liposomes is displayed in red and fluorescence from MTG as green (Figure 5). To confirm that TPP-PEG-L were localizing in the mitochondrial compartment, images in 12–14 planes at various depths within the cell, typically known as z-stacks, were taken using Z-experiment. Z-Stacked images were obtained by changing the lens position incrementally, moving the focal plane of the microscope through the cells. The center focal plane was set at the middle focusing the nucleus. The first and last planes were selected as the out-of-focus exterior of the cells. The laser scanning microscope (LSM) files were analyzed using Image *J* software. Fluorescent micrographs of red, green, and blue channels were overlaid so that the co-localization of the red fluorescence of liposomes with green fluorescence of the stained mitochondria was rendered yellow.

2.8. PTX-mediated cytotoxicity

The *in vitro* cytotoxicity of PTX delivered by PL and TPP-PEG-L was evaluated with HeLa and 4T1 cells. The cells were seeded in 96-well cell culture plates, at a density of 5×10^3 cells/well, and after the overnight incubation, the cells were treated with various concentrations of PTX in PL or TPP-PEG-L formulations diluted in complete medium. The cells were incubated for 24 h. In another study, the cells were exposed to a fixed PTX concentration of 650 μg/mL in PL and TPP-PEG-L for 12, 24, and 48 h. The cell viability after each treatment at regular time intervals was determined by the Cell Titer Blue Assay following the manufacturer's protocol. The % of cell-viability as a function of PTX concentration for 24 h study and as a function of time (12, 24, and 48 h) was plotted. Cells treated with medium were considered 100 % viable.

2.9. *In vivo* studies

2.9.1.Animals—BALB/c mice (6–8 weeks old) were purchased from Charles River Laboratories, MA, USA. All animal procedures were performed according to an animal care protocols approved by Northeastern University Institutional Animal Care and Use committee in accordance with the "Principles of Laboratory Animal care", NIH publication no. 85–23, revised in 1985. Mice were housed in groups of 5 at 19 to 23°C with a 12 h light-dark cycle and allowed free access to food and water.

2.9.2. Anti-tumor efficacy of TPP-PEG-L-PTX and PL-PTX—To assay whether the PTX-incorporated in TPP-PEG-L has improved therapeutic efficacy *in vivo* compared to

PTX in PL, a subcutaneous tumor was established by inoculating 4T1 murine mammary carcinoma cells (2×10^5) in the left flank of 6–8 week-old BALB/c mice. The time for the appearance of the tumor was usually 10–14 days. The treatment was started after the tumor reached a volume of 50–100 mm^3. The PL and TPP-PEG-L were loaded with PTX at a concentration of 1 % w/w of total lipids. The PTX dose administered to the mice was 1 mg PTX/Kg. The liposomes were diluted to a concentration of 10 mg of total lipids or 100 μg of PTX/mL of liposomal suspension so that the mice (approximately 20 g) received ~ 200 μL of liposome preparation via tail vein injection. Groups of mice were as follows: (i) Saline (the control group); (ii) PL-PTX and (iii) TPP-PEG-L-PTX (n=6 in each group). Injection via tail vein were once every 3 days (8 times) for 22 days. The tumor volume and body weight were recorded for all tumor-bearing mice for 26 days until the tumor size of animals in the control and PLPTX groups reached 1000 mm^3, after which animals were sacrificed with CO_2. The length and width of the tumors were measured by calipers and the tumor volume was calculated using the following formula: ($Width^2$ X length) / 2. The post-mortem tumor weight was taken after washing the tumors with PBS. The tumors were embedded in tissue freezing media and stored at −80 °C. For tumor histology, tumor slices (10 μM) were cryo-sectioned and stained with the terminal Deoxynucleotidyl Transferase Biotin-dUTP Nick End Labeling (TUNEL) assay following the manufacturer's protocol and examined under a fluorescence microscope equipped with green filter.

2.9.3. Statistical analysis—All data were analyzed using the one-way Student's *t*-test with unequal variances. All numerical *in vitro* data are expressed as mean ± SD, n=6. *In vivo* data are expressed as mean ± SEM, n= 6 in each group. Two-way ANOVA followed by the Bonferroni's post-hoc test were conducted for all paired groups using Graph Pad prism 4 software (GraphPad Software, Inc.; San Diego, CA). Any *p* value less than 0.05 was considered statistically significant.

3. Results

3.1. Synthesis of mitochondriotropic polymer TPP-PEG-PE

The TPP group was successfully introduced at the distal end of the PEG chain by the amide-coupling reaction between amine-functionalized NH_2-PEG-2000-PE and CTPP using the zero-length cross linker, EDCI, following the synthesis scheme shown in Figure 1. The appearance of the signal from 15 aromatic protons of the TPP group at ppm 7.69–7.84 in the NMR spectra indicated successful conjugation. The spectra was as follows (triplet, broad singlet, multiplates were abbreviated as t, bs, m, respectively): ^{1}H-NMR: ppm δ 0.88–0.91 (t, 6H, from the end-methyl group of the two lipophilic chains in the phospholipids), 1.2–1.3 (bs), 1.59 (bs), 1.9–2.0 (m), 2.27–2.31 (m), 2.53–2.88 (m), 3.10–3.70 (m), 3.80 (t), 3.9–4.0 (m), 4.16–4.18 (m), 4.36–4.40 (m), 5.2 (bm), 6.3 (bs), 7.69–7.74 (m, 7H, Ar-*H*), 7.76–7.84 (m, 8H, Ar-*H*).

3.2. Preparation and characterization of liposomes

Lipid compositions, particle size and zeta potential of prepared liposomes are shown in Table 1. Functionalized liposomes, surface-modified with TPP-PEG-PE or STPP and PTX-loaded liposomes exhibited particle sizes in the range of 145–175 nm. Figure 2A, C and D represent the particle sizes of the liposomes, that are modified with 3, 5, and 8 mole % of TPP-PEG-PE or PEG-PE. Even though there was not much difference in the average particle size of the liposomes, zeta potential of the liposomes changed significantly upon the addition of varied amount of TPP-PEG-PE or STPP. TPP-PEG-L-8 % had a slightly positive zeta potential (1.66 ± 5.49 mV), whereas TPP-PEG-L-3 and -5 % demonstrated negative zeta values (Figure 2B).

3.3. Toxicity of empty liposomes

The treatment of HeLa cells with empty TPP-PEG-L-8 % at lipid concentrations as high as 500 μg/mL for 24 h resulted in no cytotoxicity, whereas all other liposomes tested in this assay demonstrated a significant dose dependant toxicity (Figure 3). All STPP-modified liposomes were toxic with the highest observed at STPP-L-8 %. At 500 μg/mL lipid concentrations, STPP-L-1.5 % resulted in 46 ± 2 % cell viability, whereas STPP+PEG-L and STPP-L-8 % showed complete cell killing. Comparison of the cell viability of STPP +PEG-L and STPP-L indicated that PEGylation improved the cell viability with less IC_{50} values (IC_{50} for STPP-L-8 % was 83.3 ±3 μg/mL; for STPP+PEG-L, 130 ±2.5 μg/mL). This result indicated that the TPP-PEG-L do not interfere with cellular functions, while STPP, even at 1.5 mole % provoked significant cytotoxicity.

3.4. Quantification of cellular uptake of TPP-PEG-L by flow cytometry

To quantify the cellular uptake of TPP-PEG-L in HeLa cells compared to PL, we used Rh-labeled liposome preparations and measured the cell-associated fluorescence intensity by FACS. Cells treated with TPP-PEG-L containing 3 mole % of TPP-PEG-PE showed a low level of fluorescence, which was not significantly different from that after cell treatment with PL. However, the fluorescence intensity of the cells treated with TPP-PEG-L-5% and -8% was higher than that of the corresponding PL as seen by the right shift of the fluorescence intensity curve for TPP-PEG-L-treated cells in the FACS histogram (Figure 4). TPP-PEG-L-8%-treated cells showed a 1.6 fold higher geometric mean of fluorescence than cells treated with PL.

3.5. Mitochondrial targeting by Confocal Laser Scanning Microscopy (CLSM)

To investigate the mitochondrial targeting by TPP-PEG-modified liposomes, the HeLa cells were incubated with Rh-PE-labeled liposomes, and the mitochondria were stained with MTG. The appearance of yellow dots indicate the co-localization of green fluorescence from MTG and red fluorescence from liposomes. A high degree of co-localization of Rh-PE fluorescence with the mitochondrial compartment was found for TPP-PEG-L compared to PL (Figure 5). To further explore if the TPP-PEG-L were targeting to the mitochondria after successful internalization, z-stacked images (z-section thickness 0.7 μM) of cells treated with liposomes, MTG and Hoechst 33342 were taken. The z2-4 and z10-12 indicated the exterior of the cells. A high degree of yellow signal in the middle slices, z6-8, for TPP-PEG-L indicated that the TPP-PEG-L were internalized by the cells and co-localized within mitochondria (Figure 6).

3.6. PTX-mediated cytotoxicity

To explore whether the specific delivery of the therapeutic cargo to the mitochondria by TPP-PEG-PE-targeted liposomes results in improved drug action, TPP-PEG-L and PL, were loaded with PTX, and cell-killing effect of PTX in different preparations was evaluated. Results indicated that the specific delivery of PTX to the mitochondria by TPP-PEG-L elicited a time-dependant robust apoptotic response in HeLa cells which was much stronger than when delivered by PL (Figure 7). The viability of 4T1 cells was also more significantly reduced by TPP-PEG-L-PTX than by PL-PTX. After the incubation of both cells with PL-PTX or TPP-PEG-L-PTX for 24 and 48 h at a PTX dose of 650 μg/mL, the TPP-PEG-L-PTX resulted in significantly higher toxicity compared to PL-PTX. The toxicity of empty liposomes at the same lipid concentrations used for the assay (~50 μg/mL) was also determined, which indicated that the empty liposomes were not toxic to the cells after the incubation for 48 h.

3.7. Anti-tumor efficacy of TPP-PEG-L-PTX compared and PL-PTX

The efficiency of PTX delivery by mitochondria-targeted TPP-PEG-L compared to PL was determined by evaluating the anti-tumor activity of different preparations of PTX in 4T1-tumor bearing mice. Anti-tumor activity was determined by tumor volumes over 26 days (Figure 8). At a PTX dose of 1 mg/kg, TPP-PEG-L-PTX induced a significantly higher inhibition of tumor growth than PL-PTX. Although PL-PTX initially slightly reduced tumor volume compared to the untreated control, no significant decrease in tumor volume was apparent at the end of the experiment. The average tumor volume of the group treated with TPP-PEG-L-PTX was 337 ± 16 mm^3, whereas with the PL-PTX treatment it was 970 ± 77 mm^3 at the end of the experiment (Figure 8). There were no apparent toxic side-effects on overall well-being of animals. The treated animals showed no reduction in body weight over the treatment period (Figure 8C). Nuclear DNA fragmentation, the marker of apoptosis, was followed by TUNEL assay of the frozen tumor cryostat sections. The fluorescence microscopy images demonstrated significant apoptotic cell death in tumors treated with TPP-PEG-L-PTX as indicated by green fluorescence attributed to FITC-labeled TdT. Very few TUNEL-positive cells were observed in tumors injected with PL-PTX (Figure 8D).

4. Discussion

Targeting mitochondria is a promising strategy for cancer chemotherapy. Advances in the research on mitochondria have revealed that the mutation of the mitochondrial genome causes a variety of human diseases including cancer. 'Mitochondrial dysfunction is responsible for cancer'- this insight was first reported over 75 years ago by Otto Warburg [36]. He recognized that cancer cells generate excessive lactate by metabolizing glucose, but at the same time consume oxygen via mitochondrial OXPHOS. The phenomena is termed aerobic glycolysis, which may be the result of abnormal OXPHOX due to the mutations of the mitochondrial genome. Partial inhibition of OXPHOS by such genetic mutations results in reduced electron flux through the electron transport chain leading to high ROS production which serves as a mutagen for nuclear proto-oncogenes that drive nuclear replication resulting in the initiation of cancer [37]. The mitochondrial role in cancer suggested a mitochondrial targeted treatment strategy [3, 38, 39]. In this regard, the inhibition of mitochondrial ROS production, down-regulation of the anti-apoptotic mitochondria-associated protein Bcl-2 was proposed as a useful strategy for anticancer therapy [38]. PTX has been used as a potent chemotherapeutic drug and its poor water solubility has been addressed by loading this drug into various nanocarriers including liposomes [40–43]. It has been reported that the PTX, directly binds to the anti-apoptotic Bcl-2 in mitochondria and opens the mitochondrial permeability transition pore (MPTP). PTX is known to target β-tubulin and interferes with microtubule dynamics [20]. In addition to blocking the cell-cycle at the transition from metaphase to anaphase, PTX activates the intrinsic mitochondrial apoptotic pathway by reducing the mitochondrial membrane potential by opening the MPTP channels. The opening of such pores results in release of pro-apoptotic factors, such as cytochrome *C* and apoptosis-inducing factors, and in turn results in the activation of effector caspases [44]. This intriguing cascade of action results in initiation of apoptosis. It has also been reported that PTX functionally mimics the activitiy of Nur77, an orphan nuclear receptor [20]. Nur77 changes Bcl-2 function, by translocation from the nucleus to mitochondria and represents a cell-death signal. PTX mimics the binding motif of its endogenous ligand Nur and alters Bcl-2 from anti-apoptotic to pro-apoptotic. Therefore, PTX mimics the death signal mediated by Nur. This finding, that the apoptotic action of some of chemotherapeutic agents including PTX is mediated through mitochondria prompted investigation of mitochondrial targeted drug delivery strategies to improve efficacy of the anticancer therapy [29, 33, 34].

Mitochondria-targeted DDS have received a lot of attention recently [3, 28, 30, 31, 33]. This effort with emphasis on mitochondrial research has enabled investigators to identify various small molecules, such as lipophilic cations that target mitochondria [24]. In this regard, the triphenylphosphonium (TPP) cation has been found to be a potent mitochondriotropic due to its high lipophilicity and stable cationic charge. Therefore, a strategy to target bio-active molecules to mitochondria is to attach to them the TPP group [45]. However, this could result in the reduction, or complete loss of potency, due to the structural modification of the drug molecule. Therefore, the modification of drug-loaded DDS itself looked more promising [33].

Our studies aimed to develop a novel mitochondria-targeted liposomal DDS with the low non-specific toxicity noted for mitochondria-targeted STPP-L. The mitochondria-targeted TPP-PEG-L were prepared by surface modification of liposomes with the novel PEG-PE-based polymer, TPP-PEG-PE. The amphiphilic PEG-PE was introduced to drug delivery research as a polymeric surface modifier for liposomes [46]. The novel polymer, TPP-PEG-PE was obtained by modifying the PEG-PE with the TPP group at the distal end of the PEG chain. TPP-PEG-PE-modified liposomes were not toxic to the cells even at high lipid concentrations unlike STPP-L, which demonstrated significant cytotoxicity in cell culture systems. A significant difference in cytotoxicity of TPP-PEG-L and STPP-L could be explained by the fact that the stearyl moiety is not as biocompatible as the lipid phosphatidyl ethanolamine (PE) and has its own toxicity.

TPP-PEG-L associated with cancer cells better than PL as measured by the enhanced cell-associated fluorescence intensity. Research on mitochondriotropic agents has proven the fact that a compound with sufficient lipophilicity, combined with delocalized positive charge accumulates in the mitochondria due to its highly negative electric potential and membrane partitioning [24]. TPP group is highly lipophilic due to the presence of phenyl groups and the positive charge on phosphorous is delocalized into the three aromatic rings. Anchoring of TPP group on the liposomes changes liposomal lipophilicity and surface charge, which enhances its cell association and entrance to the cells by membrane partitioning.

TPP-PEG-L have also demonstrated efficient mitochondrial targeting as shown by confocal microscopy. Cells treated with fluorescently-labeled TPP-PEG-L were subjected to mitochondrial and nuclear staining, and their visualization under the confocal microscope demonstrated significantly higher degree of co-localization of TPP-PEG-L with mitochondria than for PL. There is a significant difference in cell association between TPP-PEG-L and PL. A fraction of cell-associated TPP-PEG-L was located on the cell surface, which was confirmed (Figure 6) by assessing the red fluorescence from DDS in exterior z-slices (z-2-4, z-10-11). Nevertheless, a significant fraction of TPP-PEG-L could reach the mitochondria at higher extent than PL (in Figure 6, the red signal indicated only DDS, green- only mitotracker and yellow, the co-localization of DDS with mitochondria. The center slices of the z-stacked images, which displayed strong green fluorescence from mitochondria, also displayed co-localization of green and red as yellow signal.

Next, we used TPP-PEG-L to specifically deliver the PTX to the mitochondria of cancer cell to enhance the cell killing. Our *in vitro* results clearly demonstrated that TPP-PEG-L-PTX caused significantly decreased cell viability compared to PL-PTX. Finally, we evaluated the applicability of mitochondria-targeted PTX delivery in improving its anti-tumor action *in vivo*. At the same quantity of the drug administered in experimental tumor-bearing animals as PL-PTX and TPP-PEG-L-PTX, the mitochondria-targeted preparation resulted in significantly higher tumor growth inhibition. The presence of greater apoptotic nuclei by TUNEL assay, observed in tumors treated with TPP-PEG-L-PTX than with PL-PTX

indicates that TPP-PEG-L-PTX delivered more PTX to the mitochondria. TUNEL assay indicates apoptosis as the likely mechanism of tumor suppression.

5. Conclusion

The results clearly demonstrate that liposomes modified with the novel polymer TPP-PEG-PE are non-toxic and effectively target mitochondria in cancer cells. These TPP-PEG-L can be loaded by various therapeutic agents acting on mitochondria to enhance their action. PTX-loaded TPP-PEG-L effectively kill cancer cells *in vitro* and inhibit tumor growth *in vivo* compared to PTX-loaded non-targeted PL. Such a TPP-PE-G-PE-modified DDS may serve as a useful means for mitochondria-targeted therapies.

Acknowledgments

This work was supported by the NIH grants RO1 CA121838 and RO1 CA 128486 to Vladimir P. Torchilin. We also thank Dr. William Hartner for his helpful advice in editing the manuscript.

References

1. Torchilin VP. Recent approaches to intracellular delivery of drugs and DNA and organelle targeting. Annu Rev Biomed Eng. 2006; 8:343–375. [PubMed: 16834560]
2. Shi F, Hoekstra D. Effective intracellular delivery of oligonucleotides in order to make sense of antisense. J Control Release. 2004; 97:189–209. [PubMed: 15196747]
3. Fulda S, Galluzzi L, Kroemer G. Targeting mitochondria for cancer therapy. Nat Rev Drug Discov. 2010; 9:447–464. [PubMed: 20467424]
4. Stefano JE, Hou L, Honey D, Kyazike J, Park A, Zhou Q, Pan CQ, Edmunds T. In vitro and in vivo evaluation of a non-carbohydrate targeting platform for lysosomal proteins. J Control Release. 2009; 135:113–118. [PubMed: 19146893]
5. Won YW, Lim KS, Kim YH. Intracellular organelle-targeted non-viral gene delivery systems. J Control Release. 2011; 152:99–109. [PubMed: 21255626]
6. Jensen KD, Nori A, Tijerina M, Kopeckova P, Kopecek J. Cytoplasmic delivery and nuclear targeting of synthetic macromolecules. J Control Release. 2003; 87:89–105. [PubMed: 12618026]
7. Yamada Y, Akita H, Kogure K, Kamiya H, Harashima H. Mitochondrial drug delivery and mitochondrial disease therapy--an approach to liposome-based delivery targeted to mitochondria. Mitochondrion. 2007; 7:63–71. [PubMed: 17296332]
8. Schon EA, DiMauro S. Medicinal and genetic approaches to the treatment of mitochondrial disease. Curr Med Chem. 2003; 10:2523–2533. [PubMed: 14529468]
9. Holt IJ, Harding AE, Morgan-Hughes JA. Deletions of muscle mitochondrial DNA in patients with mitochondrial myopathies. Nature. 1988; 331:717–719. [PubMed: 2830540]
10. Wallace DC. Mitochondrial diseases in man and mouse. Science. 1999; 283:1482–1488. [PubMed: 10066162]
11. King A, Selak MA, Gottlieb E. Succinate dehydrogenase and fumarate hydratase: linking mitochondrial dysfunction and cancer. Oncogene. 2006; 25:4675–4682. [PubMed: 16892081]
12. Liu X, Kim CN, Yang J, Jemmerson R, Wang X. Induction of apoptotic program in cell-free extracts: requirement for dATP and cytochrome c. Cell. 1996; 86:147–157. [PubMed: 8689682]
13. Kroemer G, Galluzzi L, Brenner C. Mitochondrial membrane permeabilization in cell death. Physiol Rev. 2007; 87:99–163. [PubMed: 17237344]
14. Galluzzi L, Joza N, Tasdemir E, Maiuri MC, Hengartner M, Abrams JM, Tavernarakis N, Penninger J, Madeo F, Kroemer G. No death without life: vital functions of apoptotic effectors. Cell Death Differ. 2008; 15:1113–1123. [PubMed: 18309324]
15. Norberg E, Orrenius S, Zhivotovsky B. Mitochondrial regulation of cell death: processing of apoptosis-inducing factor (AIF). Biochem Biophys Res Commun. 2010; 396:95–100. [PubMed: 20494118]

16. Cohen GM. Caspases: the executioners of apoptosis. Biochem J. 1997; 326(Pt 1):1–16. [PubMed: 9337844]

17. Weyland M, Manero F, Paillard A, Gree D, Viault G, Jarnet D, Menei P, Juin P, Chourpa I, Benoit JP, Gree R, Garcion E. Mitochondrial targeting by use of lipid nanocapsules loaded with SV30, an analogue of the small-molecule Bcl-2 inhibitor HA14-1. J Control Release. 2011; 151:74–82. [PubMed: 21138749]

18. Li H, Kolluri SK, Gu J, Dawson MI, Cao X, Hobbs PD, Lin B, Chen G, Lu J, Lin F, Xie Z, Fontana JA, Reed JC, Zhang X. Cytochrome c release and apoptosis induced by mitochondrial targeting of nuclear orphan receptor TR3. Science. 2000; 289:1159–1164. [PubMed: 10947977]

19. Lin B, Kolluri SK, Lin F, Liu W, Han YH, Cao X, Dawson MI, Reed JC, Zhang XK. Conversion of Bcl-2 from protector to killer by interaction with nuclear orphan receptor Nur77/TR3. Cell. 2004; 116:527–540. [PubMed: 14980220]

20. Ferlini C, Cicchillitti L, Raspaglio G, Bartollino S, Cimitan S, Bertucci C, Mozzetti S, Gallo D, Persico M, Fattorusso C, Campiani G, Scambia G. Paclitaxel directly binds to Bcl-2 and functionally mimics activity of Nur77. Cancer Res. 2009; 69:6906–6914. [PubMed: 19671798]

21. Mironov SL, Ivannikov MV, Johansson M. [Ca2+]i signaling between mitochondria and endoplasmic reticulum in neurons is regulated by microtubules. From mitochondrial permeability transition pore to Ca2+-induced Ca2+ release. J Biol Chem. 2005; 280:715–721. [PubMed: 15516333]

22. Murphy MP. Targeting lipophilic cations to mitochondria. Biochim Biophys Acta. 2008; 1777:1028–1031. [PubMed: 18439417]

23. Li L, Geisler I, Chmielewski J, Cheng JX. Cationic amphiphilic polyproline helix P11LRR targets intracellular mitochondria. J Control Release. 2010; 142:259–266. [PubMed: 19840824]

24. Horobin RW, Trapp S, Weissig V. Mitochondriotropics: a review of their mode of action, and their applications for drug and DNA delivery to mammalian mitochondria. J Control Release. 2007; 121:125–136. [PubMed: 17658192]

25. Adlam VJ, Harrison JC, Porteous CM, James AM, Smith RA, Murphy MP, Sammut IA. Targeting an antioxidant to mitochondria decreases cardiac ischemia-reperfusion injury. FASEB J. 2005; 19:1088–1095. [PubMed: 15985532]

26. Kelso GF, Porteous CM, Coulter CV, Hughes G, Porteous WK, Ledgerwood EC, Smith RA, Murphy MP. Selective targeting of a redox-active ubiquinone to mitochondria within cells: antioxidant and antiapoptotic properties. J Biol Chem. 2001; 276:4588–4596. [PubMed: 11092892]

27. Jauslin ML, Meier T, Smith RA, Murphy MP. Mitochondria-targeted antioxidants protect Friedreich Ataxia fibroblasts from endogenous oxidative stress more effectively than untargeted antioxidants. FASEB J. 2003; 17:1972–1974. [PubMed: 12923074]

28. Hoye AT, Davoren JE, Wipf P, Fink MP, Kagan VE. Targeting mitochondria. Acc Chem Res. 2008; 41:87–97. [PubMed: 18193822]

29. Biswas S, Dodwadkar NS, Sawant RR, Koshkaryev A, Torchilin VP. Surface modification of liposomes with rhodamine-123-conjugated polymer results in enhanced mitochondrial targeting. J Drug Target. 2011; 19:552–561. [PubMed: 21348804]

30. Flierl A, Jackson C, Cottrell B, Murdock D, Seibel P, Wallace DC. Targeted delivery of DNA to the mitochondrial compartment via import sequence-conjugated peptide nucleic acid. Mol Ther. 2003; 7:550–557. [PubMed: 12727119]

31. Cuchelkar V, Kopeckova P, Kopecek J. Novel HPMA copolymer-bound constructs for combined tumor and mitochondrial targeting. Mol Pharm. 2008; 5:776–786. [PubMed: 18767867]

32. Boddapati SV, Tongcharoensirikul P, Hanson RN, D'Souza GG, Torchilin VP, Weissig V. Mitochondriotropic liposomes. J Liposome Res. 2005; 15:49–58. [PubMed: 16194927]

33. Boddapati SV, D'Souza GG, Erdogan S, Torchilin VP, Weissig V. Organelle-targeted nanocarriers: specific delivery of liposomal ceramide to mitochondria enhances its cytotoxicity in vitro and in vivo. Nano Lett. 2008; 8:2559–2563. [PubMed: 18611058]

34. Patel NR, Hatziantoniou S, Georgopoulos A, Demetzos C, Torchilin VP, Weissig V, D'Souza GG. Mitochondria-targeted liposomes improve the apoptotic and cytotoxic action of sclareol. J Liposome Res. 2010; 20:244–249. [PubMed: 19883213]

35. Gabizon A, Papahadjopoulos D. Liposome formulations with prolonged circulation time in blood and enhanced uptake by tumors. Proc Natl Acad Sci U S A. 1988; 85:6949–6953. [PubMed: 3413128]
36. Warburg O. On the origin of cancer cells. Science. 1956; 123:309–314. [PubMed: 13298683]
37. Wallace DC. Mitochondria and cancer: Warburg addressed. Cold Spring Harb Symp Quant Biol. 2005; 70:363–374. [PubMed: 16869773]
38. Brandon M, Baldi P, Wallace DC. Mitochondrial mutations in cancer. Oncogene. 2006; 25:4647–4662. [PubMed: 16892079]
39. Laquintana V, Denora N, Musacchio T, Lasorsa M, Latrofa A, Trapani G. Peripheral benzodiazepine receptor ligand-PLGA polymer conjugates potentially useful as delivery systems of apoptotic agents. J Control Release. 2009; 137:185–195. [PubMed: 19374931]
40. Chen X, Wang X, Wang Y, Yang L, Hu J, Xiao W, Fu A, Cai L, Li X, Ye X, Liu Y, Wu W, Shao X, Mao Y, Wei Y, Chen L. Improved tumor-targeting drug delivery and therapeutic efficacy by cationic liposome modified with truncated bFGF peptide. J Control Release. 2010; 145:17–25. [PubMed: 20307599]
41. Saad M, Garbuzenko OB, Ber E, Chandna P, Khandare JJ, Pozharov VP, Minko T. Receptor targeted polymers, dendrimers, liposomes: which nanocarrier is the most efficient for tumor-specific treatment and imaging? J Control Release. 2008; 130:107–114. [PubMed: 18582982]
42. Yang T, Choi MK, Cui FD, Kim JS, Chung SJ, Shim CK, Kim DD. Preparation and evaluation of paclitaxel-loaded PEGylated immunoliposome. J Control Release. 2007; 120:169–177. [PubMed: 17586082]
43. Immordino ML, Brusa P, Arpicco S, Stella B, Dosio F, Cattel L. Preparation, characterization, cytotoxicity and pharmacokinetics of liposomes containing docetaxel. J Control Release. 2003; 91:417–429. [PubMed: 12932719]
44. Bhalla KN. Microtubule-targeted anticancer agents and apoptosis. Oncogene. 2003; 22:9075–9086. [PubMed: 14663486]
45. Smith RA, Porteous CM, Gane AM, Murphy MP. Delivery of bioactive molecules to mitochondria in vivo. Proc Natl Acad Sci U S A. 2003; 100:5407–5412. [PubMed: 12697897]
46. Klibanov AL, Maruyama K, Torchilin VP, Huang L. Amphipathic polyethyleneglycols effectively prolong the circulation time of liposomes. FEBS Lett. 1990; 268:235–237. [PubMed: 2384160]

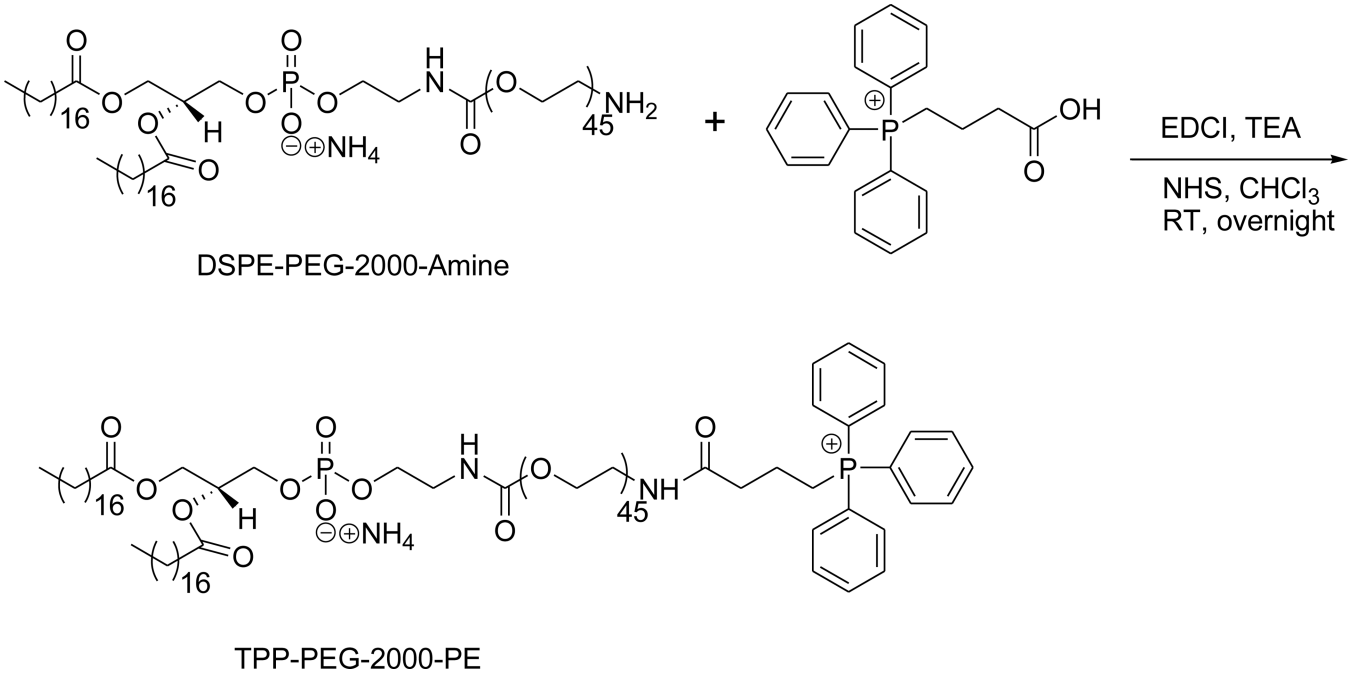

Figure 1.
Synthesis scheme for the preparation of TPP-PEG-PE.

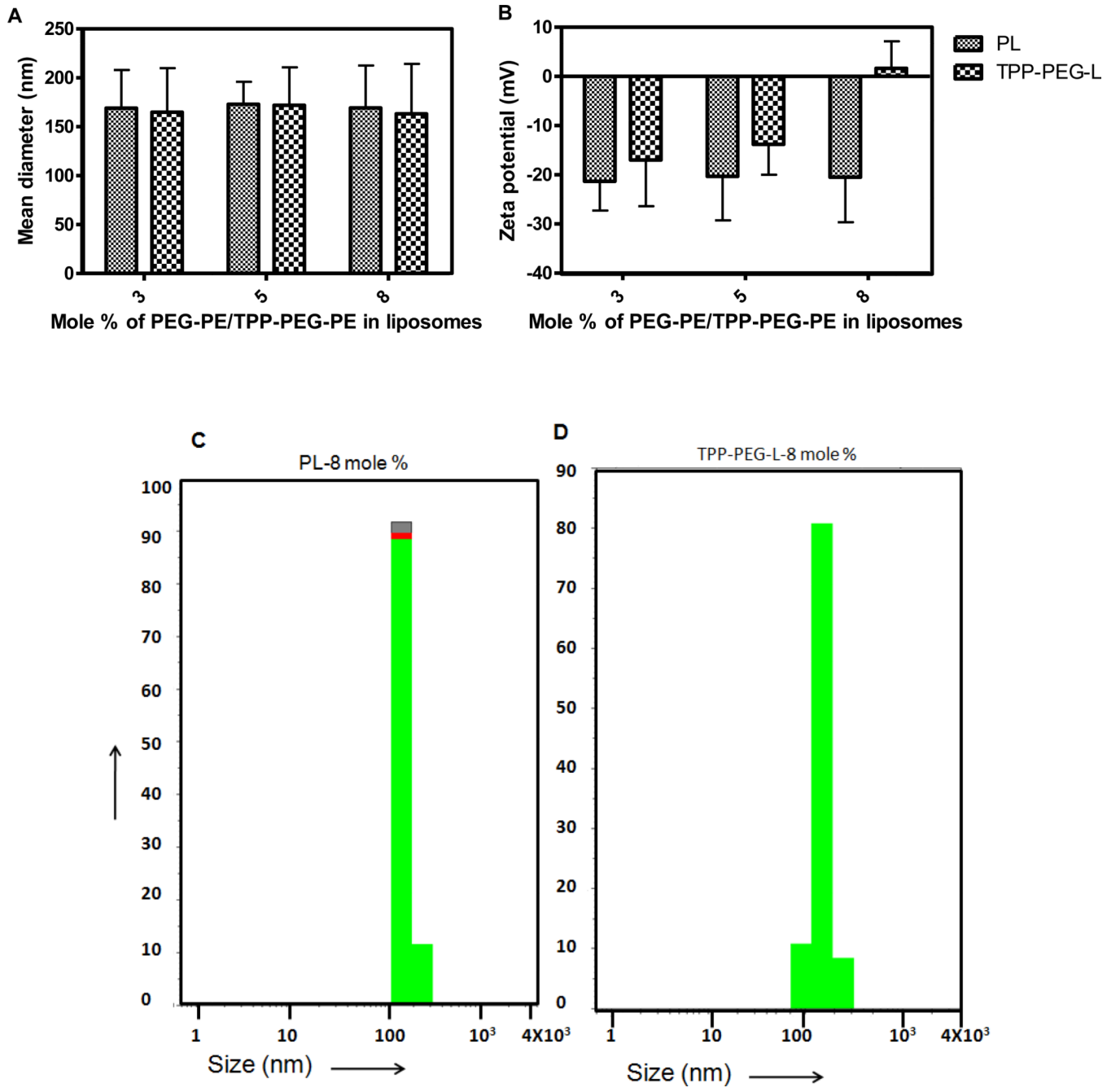

Figure 2.

Physico-chemical characterization of TPP-modified liposomes. A. Size of liposomes containing varied mole % of TPP-PEG-PE or PEG-PE; B. Zeta potential of TPP-PEG-L and PL; C and D. Particle size distribution of PL modified with 8 mole % PEG-PE and TPP-PEG-PE.

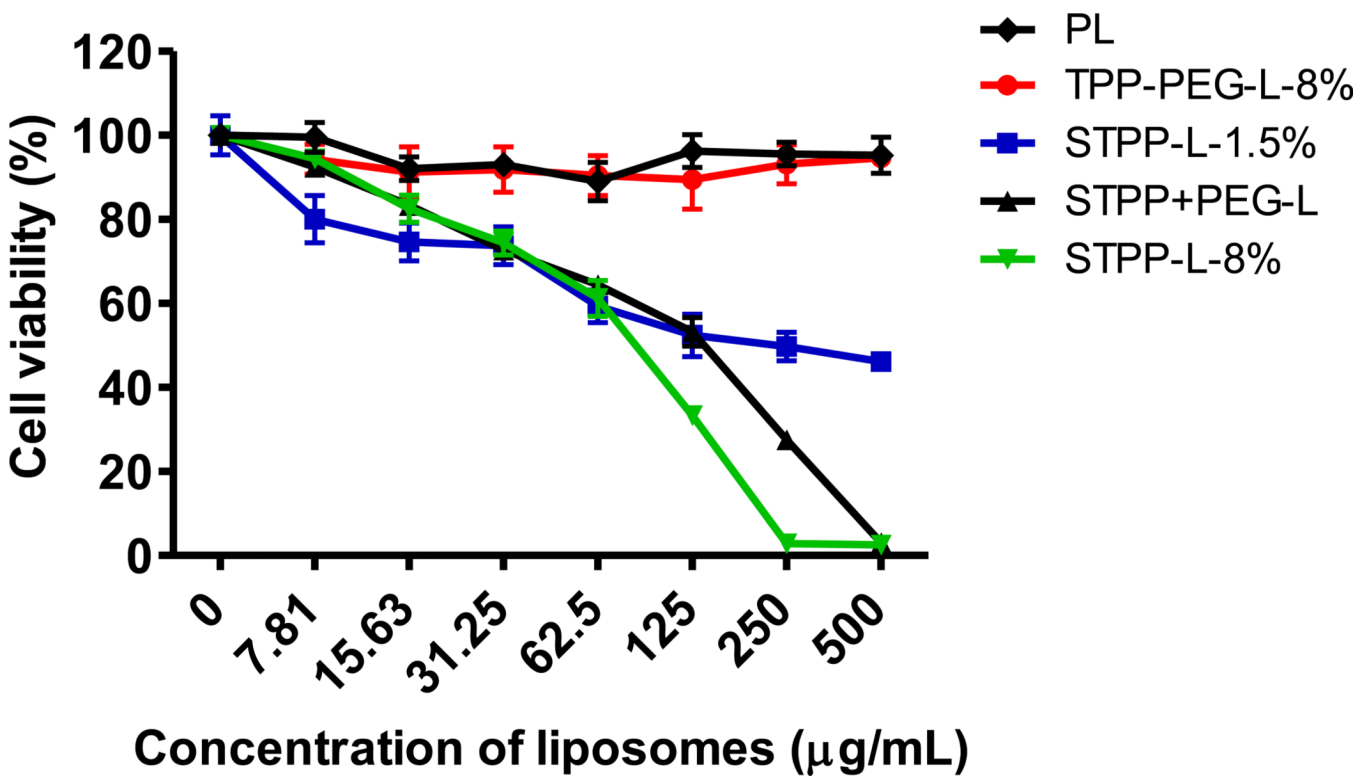

Figure 3.
Survival of HeLa cells treated with TPP-modified liposomes. The cells were incubated with liposomes for 24 h, before measurement of cell-viability. TPP-PEG-L-8% were non-toxic, even at high lipid concentrations, whereas the liposomes modified with STPP induced cell death, starting at low lipid concentrations.

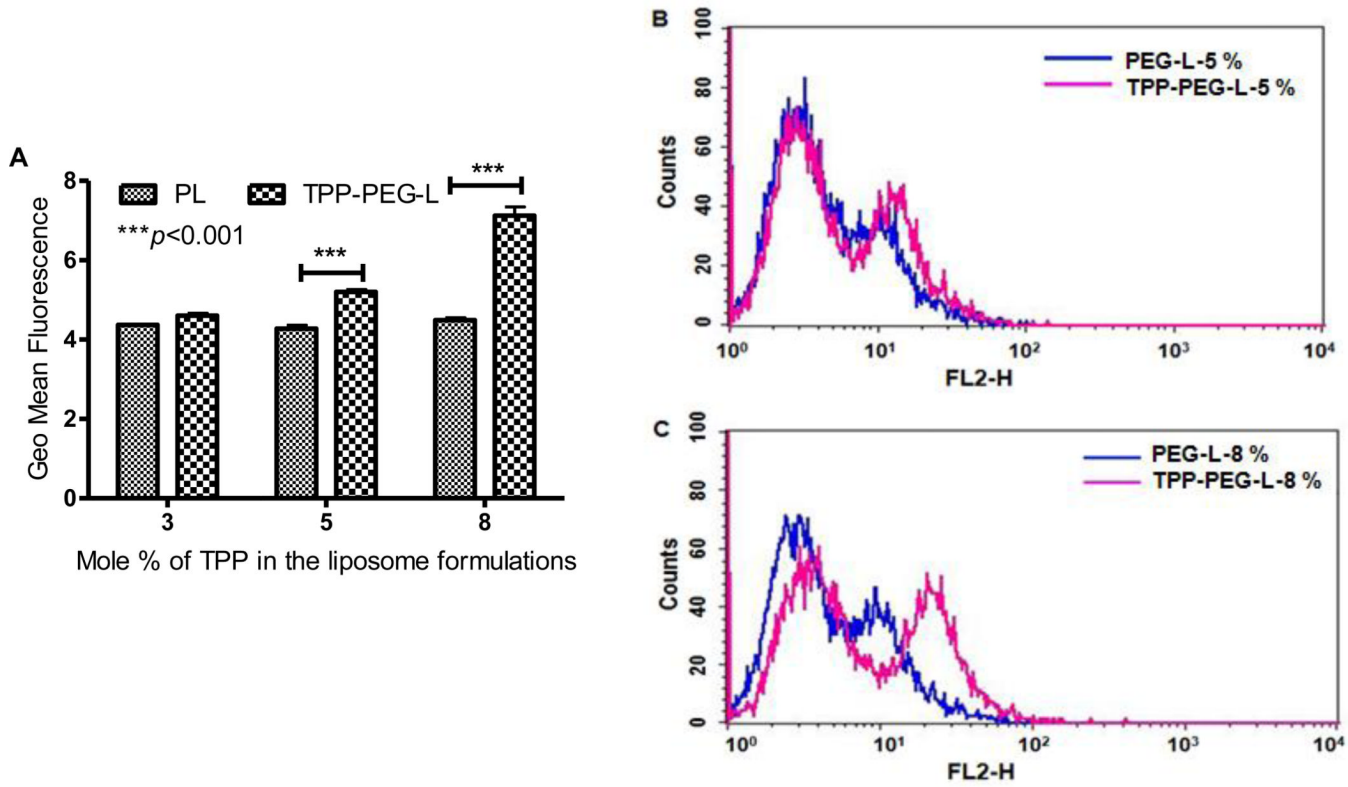

Figure 4.

Quantification of the cellular uptake of TPP-PEG-L and PL modified with different mole % of TPP-PEG-PE or PEG-PE by HeLa cells by FACS analysis. HeLa cells were treated with Rh-PE-labeled TPP-PEG-L and PL for 1 h at 37 °C. A. The geometric mean of fluorescence from three separate experiments was obtained by performing statistical analysis using Cell Quest Pro software. Geometric means of the fluorescence obtained from three separate experiments were plotted. The data represents mean ± SD, n=3. ($p<0.001$, analyzed by the Student's t-test). B and C, histogram plots show the relative uptake levels of PL and TPP-PEG-L, presented as fluorescence intensity by FACS analysis. The PL and TPP-PEG-L were modified with 5 (B) and 8 (C) mole % of TPP-PEG-PE and PEG-PE, respectively.

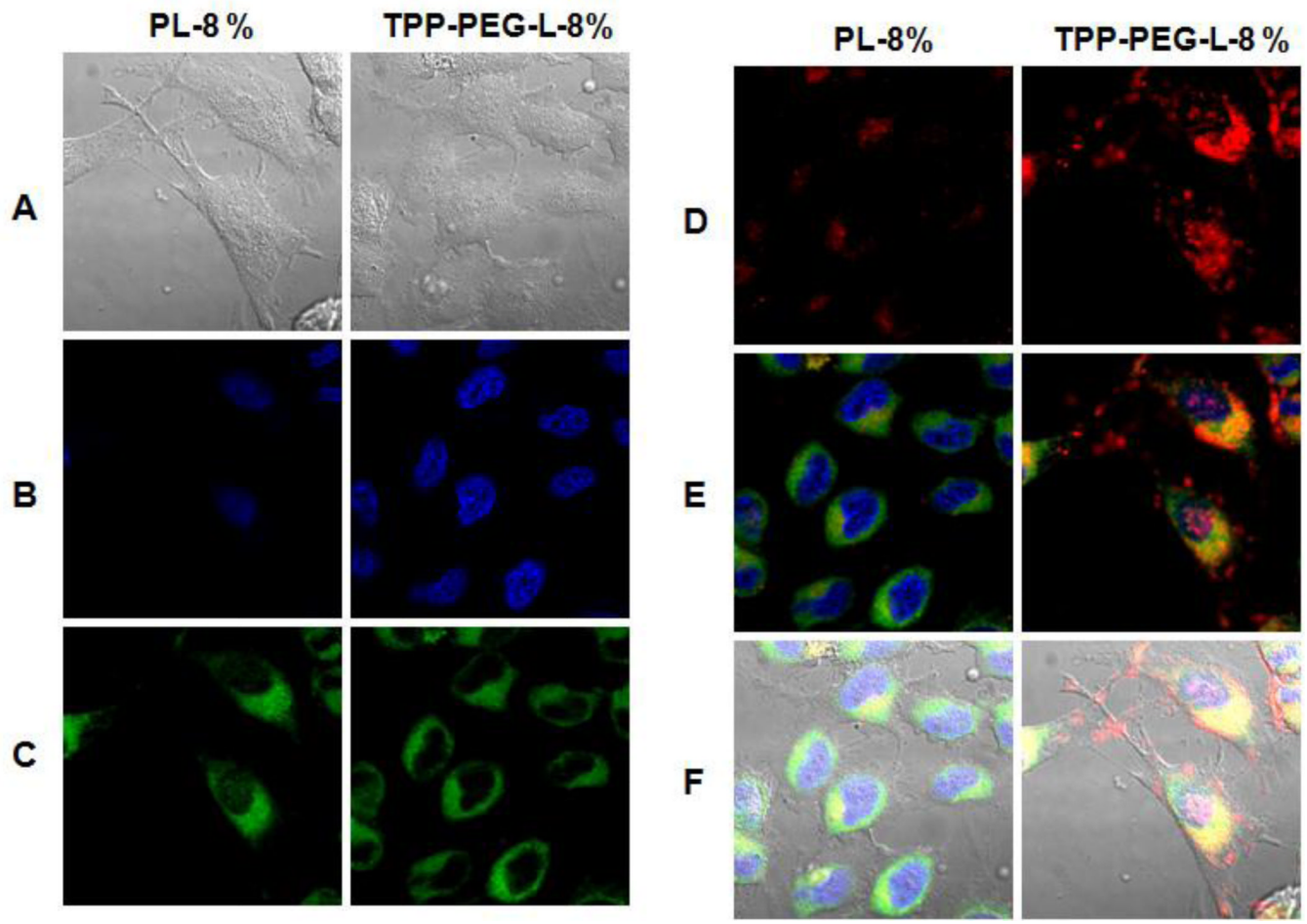

Figure 5.

Mitochondrial localization of fluorescently-labeled TPP-PEG-L compared to PL by confocal laser scanning microscopy. HeLa cells were incubated with Rh-PE-labeled TPP-PEG-L-8% and PL for 18 h and then stained with MTG and Hoechst 33342. Yellow spots in the merged pictures denote the co-localization of the liposomes within mitochondrial compartments. A. Bright field images; B. Images of nuclei stained with Hoechst; C. Mitochondria staining with MTG; D. Uptake of Rh-labeled liposomes; E. Merged picture without DIC; F. Merged picture of all (A).

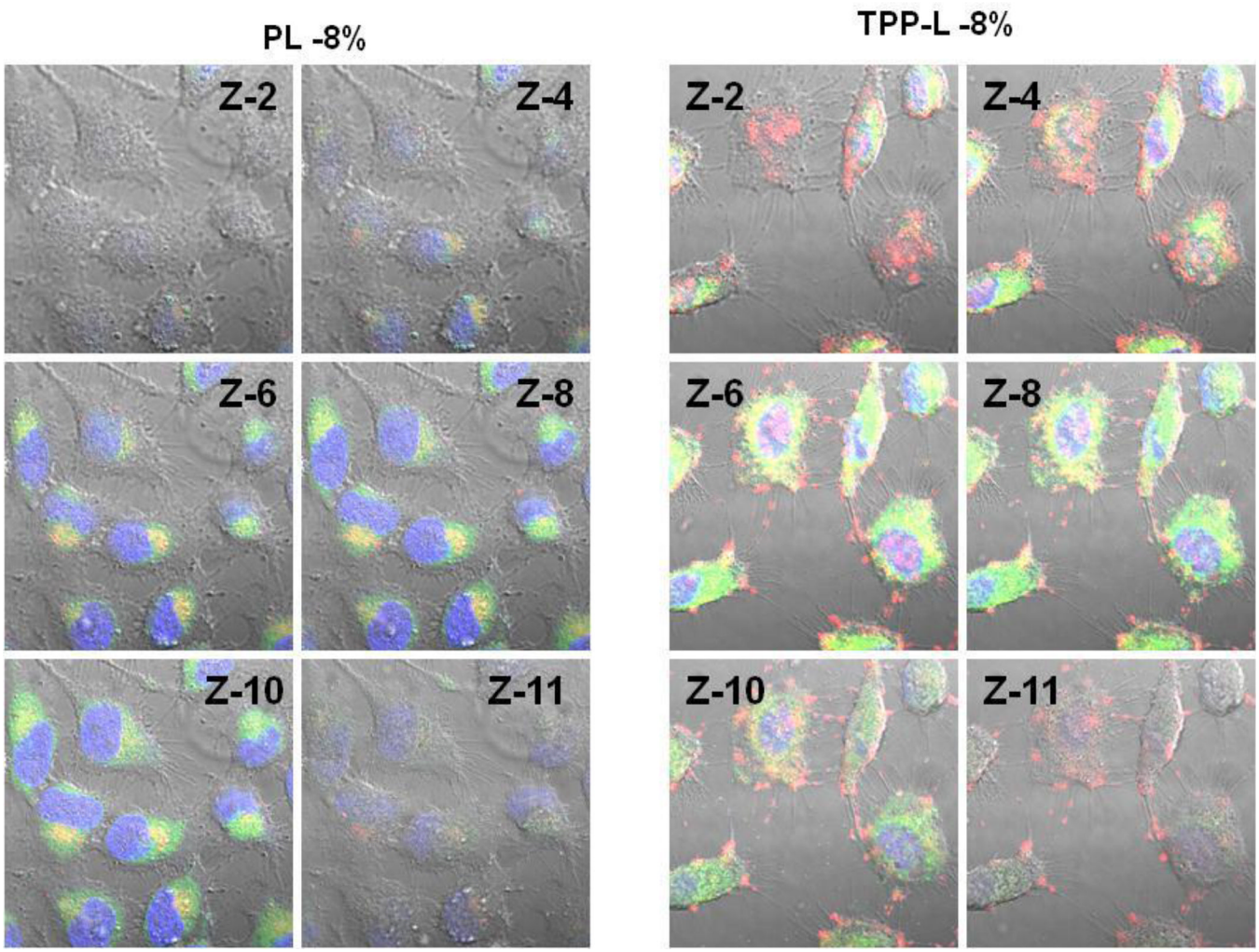

Figure 6.

Montage of z-slices obtained with confocal microscopy. The HeLa cells were incubated with Rh-labeled PL and TPP-PEG-L-8 % (red channel, laser 540 nm) for 18 h before analysis of their mitochondrial co-localization using MTG (green channel, Laser 490 nm). Hoechst 33342 was used for staining nuclei (blue channel, Laser 405 nm). Merged images of selected slices (z-2,4,6,8,10,11) from a total of 12 slices (slice thickness. 0.75 μM) are displayed.

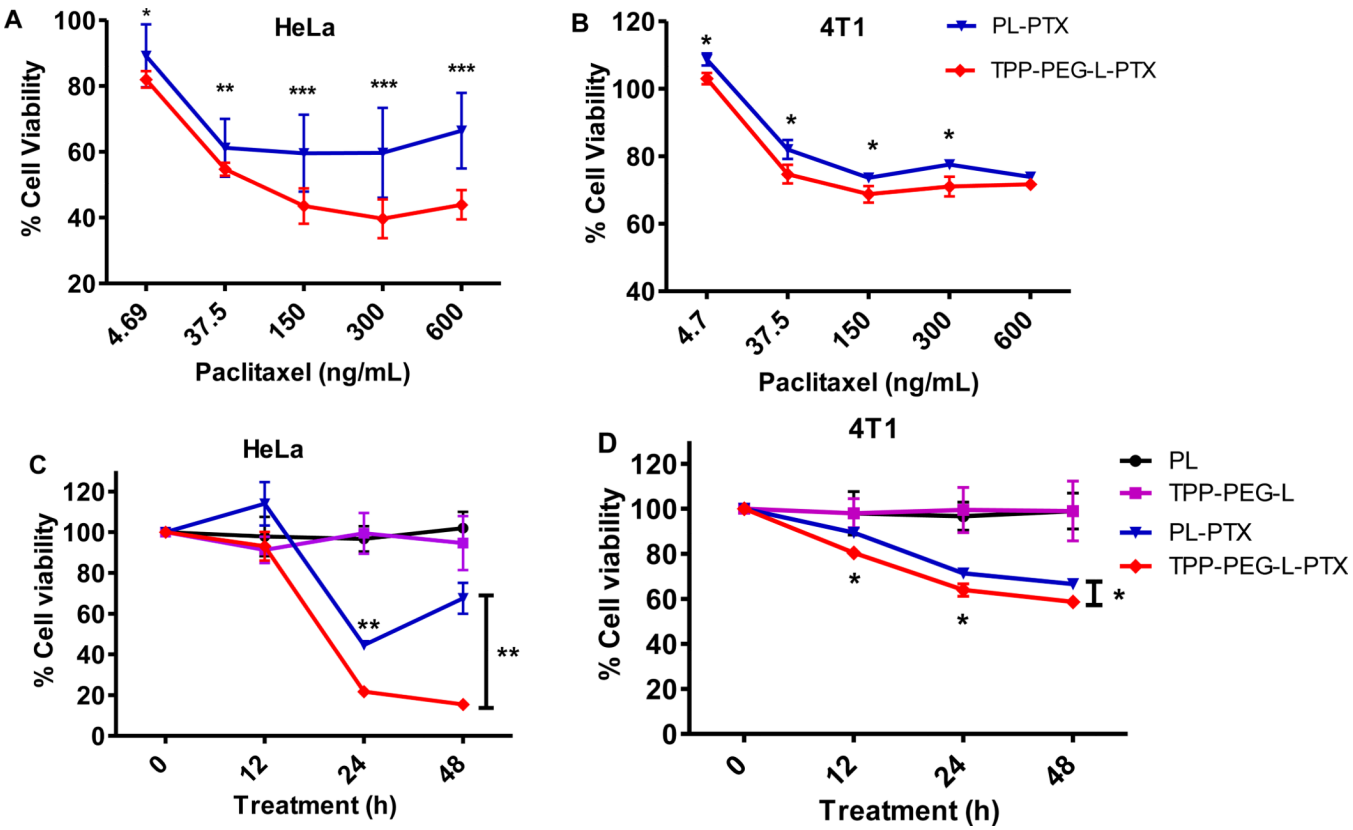

Figure 7.

Cytotoxicity of different preparations of PTX towards HeLa and 4T1 cells. A and B: HeLa and 4T1 cells were incubated with PL-PTX and TPP-PEG-L-PTX loaded with varied concentration of PTX (the highest PTX dose, 600 ng/mL) for 24 h. C and D: Cells were treated with PTX in different preparations at 650 ng/mL concentration for 48 h. Cell viability was measured at 12, 24 and 48 h. TPP-PEG-L-PTX resulted in significantly greater cytotoxicity than PL-PTX in both the cell lines. Empty PL and TPL used at the same lipid concentration as PL-PTX and TPP-L-PTX (50 μg/mL) were non-toxic (C and D). The data are mean ± SD, averaged from three separate experiments. *, ** and *** indicate $p<0.05$, $p<0.01$ and $p<0.001$ respectively, Student's t-test.

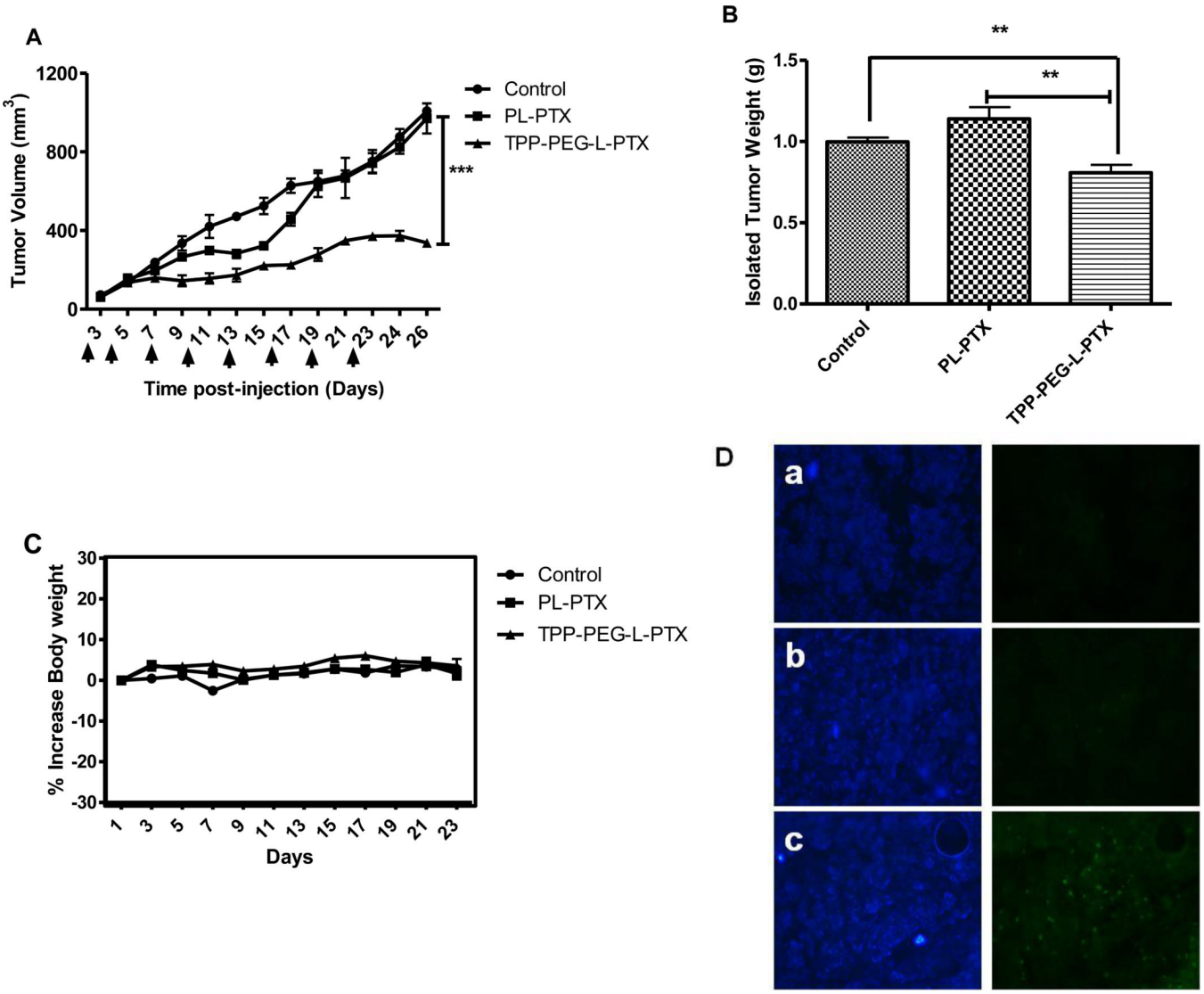

Figure 8.

In vivo therapeutic efficacy of PTX-loaded mitochondria-targeted liposomes (TPP-PEG-L-PTX) in murine breast adenocarcinoma cell (4T1)-implanted BALB/c mice. Mice bearing 4T1-tumors received 8 i.v. injections of PTX (in PL or TPP-PEG-L-8 %) via the tail vein as indicated by the arrows. (A), Tumor growth as a function of time; saline treatment was used as control. TPP-PEG-L-PTX induced statistically significant tumor growth inhibition as compared to PL-PTX and control. (B), Postmortem tumor weights from the groups treated with TPP-PEG-L-PTX, PL-PTX or saline. (C), % increase in body weights of mice as a measure of systemic toxicity; data shown in all three graphs are expressed as mean ± SEM of n= 6 per treatment group. Overall stability in body weight was observed during the treatment period indicating no systemic toxicity of the liposomal preparations. (*, ** and *** indicate $p < 0.05$, 0.001 and 0.0001, Student's t-test). (D). Detection of apoptotic cells in frozen tumor sections, determined by TUNEL assay and visualized by fluorescence microscopy. The left panel shows the sections stained with Hoechst 33342 and the right panel shows the TUNEL staining. Control (PBS treatment) (a), PL-PTX (b), and TPP-PEG-L-PTX (c). Magnification- 20× objective. TPP-PEG-L-PTX induced significantly more apparent apoptosis in tumor than PL-PTX.

Table 1

The lipid composition, size, and zeta potential of liposomes.

Liposomes	Composition (% of mole)						Size (nm)	Zeta potential (mV)
	EPC	Chol	TPP-PEG-PE	PEG-PE	STPP	PTX*		
TPP-PEG-L- 3%	67	30	3	-	-	-	164.8 ± 45.1	−17 ± 9.4
TPP-PEG-L- 5%	65	30	5	-	-	-	172.0 ± 38.8	−13.8 ± 6.2
TPP-PEG-L- 8%	62	30	8	-	-	-	163.3 ± 50.9	1.66 ± 5.5
PL- 3%	67	30	-	3	-	-	169.1 ± 38.9	−21.3 ± 5.9
PL- 5%	65	30	-	5	-	-	173.1 ± 22.8	−20.3 ± 8.9
PL- 8%	62	30	-	8	-	-	169.3 ± 43.3	−20.5 ± 9.2
STPP-L- 1.5%	68.5	30	-	-	1.5	-	164.5 ± 58.8	±
STPP-L- 8%	62	30	-	-	8	-	175.4 ± 56.0	±
STPP+PEG-L	54	30	-	8	8	-	145.3 ± 46.5	−4.9 ± 8.2
PL-PTX	62	30	-	8	-	1	163.0 ± 37.6	−18.8 ± 1.3
TPP-PEG-L-PTX	62	30	8	-	-	1	159.8 ± 39.0	1.1 ± 0.7

* weight % of total lipid